Harmonic Cut and Regularized Centroid Transform for Localization of Subcellular Structures *

Qing Yang and Bahram Parvin
Computing Sciences
Lawrence Berkeley National Laboratory
Berkeley, CA 94720

Abstract

Two novel computational techniques, harmonic cut *and* regularized centroid transform*, are developed for segmentation of cells and their corresponding substructures observed with an epi-fluorescence microscope. Harmonic cut detects small regions that correspond to subcellular structures. These regions also affect the accuracy of the overall segmentation. They are detected, removed, and interpolated to ensure continuity within each region. We show that interpolation within each region (subcellular compartment) is equivalent to solving the Laplace equation on a multi-connected domain with irregular boundaries. The second technique, referred to as the regularized centroid transform, aims to separate touching compartments. This is achieved by adopting a quadratic model for the shape of the object and relaxing it for final segmentation.*

Index terms: segmentation, scale-space, regularization, vector field

1. Introduction

As an important tool in computational biology, cell segmentation provides the basis for population studies, model validation, protein expression and uptake studies at a particular subcompartment[7, 1, 2, 5]. In general, reliable segmentation is hard since images are noisy (both random and speckle noise), cellular stain is heterogeneous, and various compartments could overlap in the sample. This paper focuses on automated segmentation of cells and their subcompartments, imaged with a confocal microscope and on a fixed focal plane, e.g., segmentation is limited to 2D images. Segmentation from 2D images is slightly more difficult than 3D images due to inherent lack of 3D content and ambiguities that originate from lack of information. Figure 2(a) shows an example of a population of cells that is imaged with a confocal microscope. Thresholding [8] and edge detection are not sufficient for delineating them from each other. In addition, notice that there are a significant number of internal structures in each nucleus. Our approach is model based, assumes an ellipsoidal model for the gross shape of the cell, which is not expressed as a parametric model, and does not rely on the user to provide an initial seed point for initial segmentation. Although the proposed techniques have been applied for localizing cells, we suggest that they are generic tools for early vision and blob detection.

The proposed computational protocol, as shown in Figure 1, is layered and involves filtering for noise and internal structures followed by grouping of iso-intensity pixels into their local centroid. In this system, noise and internal substructures are detected with elliptic features. These elliptic features are then removed and interpolated with harmonic cut. At this step of the computational process, each object of blob is represented with a smooth surface. Objects that are touching one another are grouped according to their centroid and partitioned from the computed vector field.

Organization of this paper is as follows. Section 2 provides a summary of the method for detecting elliptic features. Section 3 outlines details of the harmonic cut and its solution with the Laplacian. Sections 4-5 present the regularized centroid transform and its implementation. Section 6 concludes the paper.

2. Elliptic Regions

Let $I_0(x, y)$ be the original image. In the linear (Gaussian) scale space, its representation at scale σ is given by

$$I(x, y; \sigma) = G * I$$

*Research was funded by the Director of the Lawrence Berkeley National Laboratory, Medical Science Division, and the Mathematical, Information, and Computing Sciences Division of the U.S. Department of Energy under Contract No. DE-AC02-76SF00098 with the University of California. The publication number is LBNL-50179. Email: qyang@media.lbl.gov. Web site is: http://vision.lbl.gov.

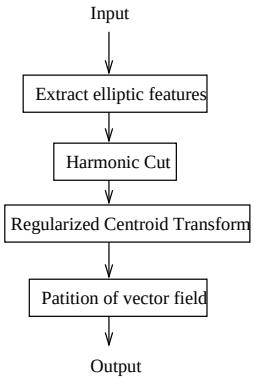

Figure 1. System diagram.

where G is the Gaussian kernel. In the rest of the paper, $I(x, y; \sigma)$ will be simply denoted as $I(x, y)$. Classification of bright and dark regions (speckled area) in the blob can then be achieved through analyzing the Hessian

$$H(x, y) = \begin{pmatrix} I_{xx} & I_{xy} \\ I_{xy} & I_{yy} \end{pmatrix}$$

Bright elliptic regions can then be defined as the set of points satisfying the following conditions: $I_{xx} < 0$, $I_{yy} < 0$ and $I_{xx}I_{yy} - I_{xy}^2 > 0$, which mean that both eigenvalues of the Hessian matrix are negative, or in other words, $H(x, y)$ is negative definite. In scale-space theory [4], $I_{xx}I_{yy} - I_{xy}^2$ is referred to as the elliptic feature.

3. Harmonic Cut

The next step of the computational process is to remove small elliptic regions from the cell and interpolate their region. This is essentially a noise removal step, however, our data set has both random noise (CCD noise) and speckle noise (internal structures within the cell). The 2D case is complex because the boundary of the region to be removed is often noisy and irregular, and it is not clear whether simple techniques such as propagating intensity based on distance transform will have desirable properties. One way to ensure continuity is to regularize the solution by extending the 1D solution to 2D or by minimizing the following functional:

$$\frac{1}{2}\iint_D I_x^2 + I_y^2 dx dy \qquad (1)$$

where D is the region to be removed, that is to say, $I(x, y)$ is supposed to be unknown in D. The Euler-Lagrange solution to this optimization problem is the Laplace equation:

$$\nabla^2 I = I_{xx} + I_{yy} = 0 \qquad (2)$$

with the Dirichlet boundary condition $I|_{\partial \bar{D}}(x, y)$, the restriction of the original image on the boundary of D's complement $\bar{D} = \Omega - D$ where Ω is the domain of definition of the entire image. Equation (2) defines a 2-dimensional harmonic function on the region to be removed, and thus we call this method "harmonic cut".

In the actual implementation, a small scale is selected and elliptic features are detected. These features correspond to either noise or tiny substructures (approximately 20 pixels) on the nuclei. The corresponding regions are subsequently interpolated with a harmonic function. Figure 2(b) shows detected elliptic features at scale $\sigma = 2$, where these bright dots, inside nuclei, are known to be chromatin. Figure 2 shows the result of the harmonic cut step by step.

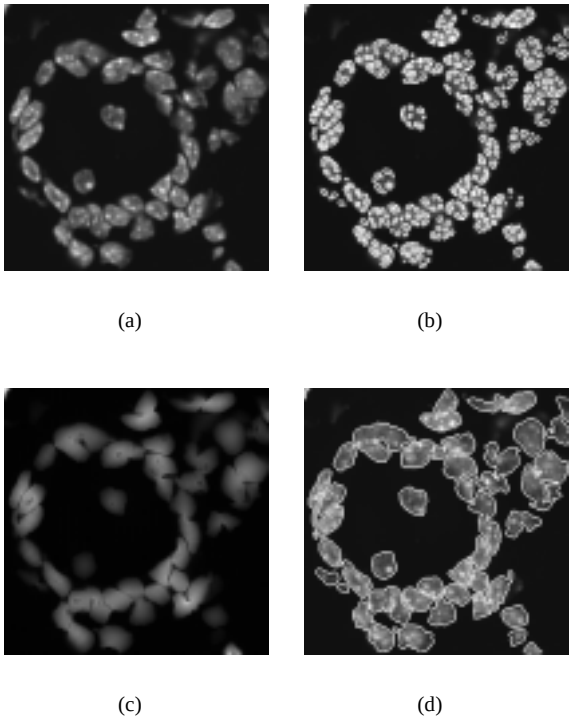

Figure 2. Detection of elliptic features and their interpolation with harmonic cuts: (a) The original image; (b) edges of bright elliptic features at scale $\sigma = 2$; (c) harmonic cut on features in (b); (d) displaying edge of (c) on the original image.

Harmonic functions are those functions that satisfy the Laplace equation. Since any non-constant harmonic function has no maximum or minimum value inside the region in which it is defined, if we remove one region and replace it with the harmonic function defined by its boundary, there is no local minimum/maximum in the removed region. Hence, *the harmonic cut can remove all local singularities.*

Therefore the harmonic cut satisfies *causality* introduced by Koenderink [3, 4] because of the inherent properties of harmonic functions.

4. Regularized Centroid Transform

At this stage of the computational process, each cell is represented with a smooth surface corresponding to each of its subcompartments. The next step of the process is to separate objects that are grouped together into a clump, e.g., touching one another. This is achieved using *Regularized Centroid Transform* (RCT).

The basic idea for the RCT technique is to map vectors originating from the boundary of an ellipse to its centroid. If these vectors can be computed, then the entire boundary can be grouped together. This is true for both boundaries and their *interior* points, e.g., grouping utilizes not only the edges but also the region information. The main issue is that centroids are unknown and that there are many centroids in the image. This is resolved by computing a vector field that can then be used to partition touching objects.

4.1. Local centroids

Let $I(x, y)$ be the original intensity image. At each point (x_0, y_0), its equal-height contour is defined by $I(x, y) = I(x_0, y_0)$. Expanding and truncating the above equation using Taylor's series, we have the following estimation:

$$I_x u + I_y v + \frac{1}{2}[I_{xx}u^2 + 2I_{xy}uv + I_{yy}v^2] = 0 \quad (3)$$

where $u = x - x_0$ and $v = y - y_0$, or in the standard form

$$\frac{1}{2} w^T H w + b^T w = 0 \quad (4)$$

where $H = \begin{pmatrix} I_{xx} & I_{xy} \\ I_{xy} & I_{yy} \end{pmatrix}_{(x_0, y_0)}$ is the Hessian matrix, $b = (I_x, I_y)^T_{(x_0, y_0)}$ is the gradient of intensity, $w = (u, v)^T$ is the centroid in the local coordinate system. Recall that the centroid of the quadratic curve defined by Eq. (4) satisfies the following linear constraint: $Hw + b = 0$. If H is non-singular, then the centroid can be determined directly; i.e., $w = -H^{-1}b$. However, this is not always true, and in general, the zero set defined by $\begin{vmatrix} I_{xx} & I_{xy} \\ I_{xy} & I_{yy} \end{vmatrix} = I_{xx}I_{yy} - I_{xy}^2 = 0$ is non-trivial, and can be further classified into two categories:

- Uniform regions that correspond to zero intensity gradient of the image with the result that there is no information to estimate the centroid, and
- Elliptic features that occur in non-uniform regions.

4.2. Regularized representation

The limitation of the local centroid technique is due to the singularities of the Hessian. From the computational stability point of view, nearby points cannot be computed reliably either. Therefore formulation of the centroid transform is ill-posed [6], and needs to be regularized. Let the centroid at (x, y) be denoted by $(u(x, y), v(x, y))^T$, then the regularized model can be expressed as

$$\begin{aligned} \min E(u, v) &= \tfrac{1}{2}\iint (I_{xx}u + I_{xy}v + I_x)^2 \\ &+ (I_{xy}u + I_{yy}v + I_y)^2 \\ &+ \alpha(u_x^2 + u_y^2 + v_x^2 + v_y^2)dxdy \end{aligned} \quad (5)$$

where the first and second terms are the error of estimation, the third term is the smoothness constraint, and $\alpha(> 0)$ is the weight factor. We refer to the solution of Equation (5) as the *regularized centroid transform* (RCT). The key ideas and properties of RCT are that: (1) the transform is a vector instead of a scalar field, (2) the vector field represents the displacement to the centroid in the x and y directions, respectively, (3) the vector field is dense everywhere and is regularized under the smoothness constraint, and (4) RCT is an intermediate step toward final segmentation.

The Euler-Lagrange equations of the variational problem of Eq. 5 are

$$\begin{cases} I_{xx}(I_{xx}u + I_{xy}v + I_x) + I_{xy}(I_{xy}u + I_{yy}v + I_y) - \\ \alpha(u_{xx} + u_{yy}) = 0 \\ I_{xy}(I_{xx}u + I_{xy}v + I_x) + I_{yy}(I_{xy}u + I_{yy}v + I_y) - \\ \alpha(v_{xx} + v_{yy}) = 0 \end{cases} \quad (6)$$

The boundary conditions for solution of the above PDEs are based on Neumann boundary conditions: $\begin{cases} \frac{\partial u}{\partial \mathbf{n}} = 0 \\ \frac{\partial v}{\partial \mathbf{n}} = 0 \end{cases}$ where $\mathbf{n}$ is the normal vector to the boundary. It is easy to show that its computational complexity is of the same order as the linear diffusion.

5. Partitioning Vector Field

The final step of segmentation is to compute the partition of a vector field corresponding to RCT. Consider an autonomous system of differential equations

$$\begin{cases} \frac{dx}{dt} = u(x, y) \\ \frac{dy}{dt} = v(x, y) \end{cases} \quad (7)$$

where $u(x, y)$ and $v(x, y)$ are the two components of RCT. We can partition RCT in the following way. Every non-singular pixel can be repeatedly moved to a new position by solving Equation (7), and every singular point is in fact a fixed point. As a result, those points that move to the same singular point can be grouped together.

We can define an *RCT energy function* as the arclength of the trajectory. Figure 3 compares the RCT energy function and the classic distance transform, which is often used for further segmentation. It is clear that the RCT map is smoother and well focused. Figure 4 shows final segmentation results for two fields of cells. We have applied our technique to 68 images with a total of 2417 cells, and 61 cells were incorrectly segmented. These images can be found at *http://vision.lbl.gov/Projects/bioinformatic/images.html*.

6. Conclusion

This paper has outlined a layered computational technique to delineate overlapping nuclei and to extract their internal substructures. The first step of the process is removal of random and speckled (internal substructure) noise, which are subsequently interpolated with harmonic cut. The next step of the process delineates overlapping regions through a novel process that we call regularized centroid transform (RCT). Our approach has been applied to analysis of images obtained through a confocal microscope, and it is currently in production use. It is possible for the proposed method to produce incorrect segmentation, however, this is due to the incomplete amount of information that is present at a given focal plane. We suggest that RCT is a generic blob detection and separation technique that can be used as a generic tool for early vision problems.

References

[1] G. Cong and B. Parvin. Model-based segmentation of nuclei. In *CVPR99*, pages I:256–261, 1999.

[2] A. Garrido and N.P. de la Blanca. Applying deformable templates for cell image segmentation. *PR*, 33(5):821–832, May 2000.

[3] J.J. Koenderink. The structure of images. *Biol. Cybern.*, 50:363–370, 1995.

[4] T. Lindeberg. Scale-space theory: A basic tool for analyzing structures at different scales. *Journal of Applied Statistics*, pages 225–270, 1994.

[5] S. Sclaroff and L. Liu. Deformable shape detection and description via model-based region grouping. *PAMI*, 23(5):475–489, May 2001.

[6] A.N. Tikhonov. The regularization of ill-posed problems. *Dokl. Akad. Nauk.*, SSR 153(1):49–52, 1963.

[7] H.S. Wu, J. Barba, and J. Gil. A parametric fitting algorithm for segmentation of cell images. *IEEE Trans. on Biomedical Engineering*, 45(3):400–7, 1998.

[8] K. Wu, D. Gauthier, and M.D. Levine. Live cell image segmentation. *IEEE Trans. on Biomedical Engineering*, 42(1):1–12, 1995.

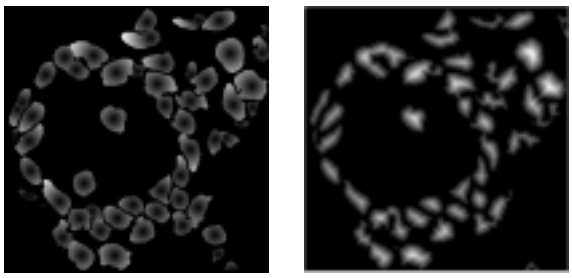

(a) (b)

Figure 3. Comparison of RCT and distance function energy map: (a) RCT energy function; (b) distance transform.

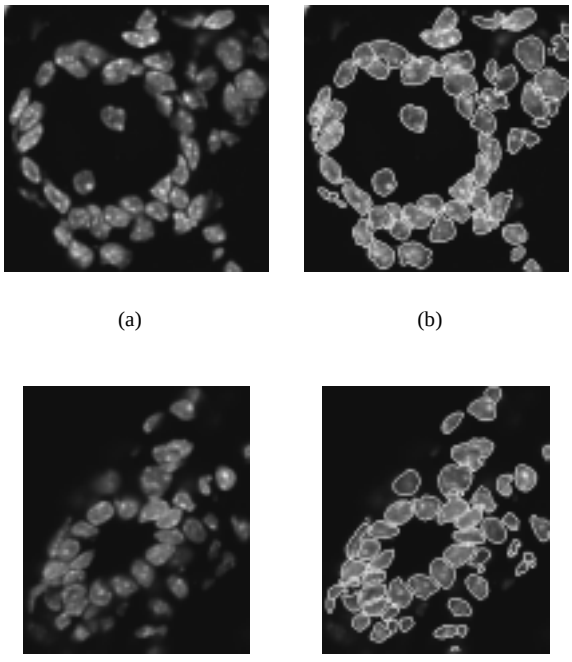

(a) (b) (c) (d)

Figure 4. Segmentation of two fields of cells.